Proceedings of the ASME 2010 3rd Joint US-European Fluids Engineering Summer Meeting and 8th International Conference on Nanochannels, Microchannels, and Minichannels
FEDSM-ICNMM2010
August 1-5, 2010, Montreal, Canada

FEDSM-ICNMM2010-30911

IMPLICATIONS OF CONTACT LINE DYNAMICS ON TAYLOR BUBBLE FLOW MORPHOLOGY

Alexandru Herescu*
Jeffrey S. Allen†
Mechanical Engineering – Engineering Mechanics
Michigan Technological University
1400 Townsend Drive
Houghton, Michigan 49931

ABSTRACT

Film deposition experiments are performed in circular glass capillaries of 500 μm diameter. Two surface wettabilities are considered, contact angle of 30° for water on glass and of 105° when a hydrophobic coating is applied. It was observed that the liquid film deposited as the meniscus translates with a velocity U presents a ridge that also moves in the direction of the flow. The ridge is bounded by a contact line moving at a velocity U_{CL} as well as a front of velocity U_F, and it translates over the deposited stagnant film. The behavior of the ridge presents striking dissimilarities when the wettability is changed. Both U_{CL} and U_F are approximately twice as large for the non-wetting case at the same capillary number Ca. The Taylor bubbles forming due to the growth of the ridge are also differentiated by wettability, being much shorter in the non-wetting case. The dynamics of the contact line is studied experimentally and a criterion is proposed to explain the occurrence of a shock at the advancing front of the ridge. The hydraulic jump cannot be explained by the Froude condition of shock formation in shallow waters, or by an inertial dewetting of the deposited film. For a dynamic contact angle of $\theta_d = 6°$ and according to the proposed criterion, a hydraulic jump forms at the front of the ridge when a critical velocity is reached.

*aherescu@mtu.edu
†Corresponding author: jstallen@mtu.edu

Nomenclature

e	Deposited film thickness
h	Ridge film thickness
h_R	Non-dimensional deposited film thickness
l	Ridge half-width
L	Transition length
R	Radius of curvature, ridge
Ca	Capillary number
Ca^*	Critical Capillary number
c	Shock velocity
U	Meniscus velocity
U_{CL}	Contact line velocity
U_F	Wave front velocity
V_1	Film velocity
V_C	Critical velocity
μ	Viscosity
ρ	Mass density
σ	Surface tension
θ	Dynamic contact angle
ΔP	Laplace pressure
$_{wet}$	Wetting
$_{nonwet}$	Non-wetting

Introduction

Taylor bubble flow is defined as finite length gas bubbles longer than the tube diameter alternating with liquid plugs. The study of film deposition (which represents the infinite bubble case) is a necessary step in understanding the interface behavior associated with the Taylor bubble flow regime. Fairbrother and Stubbs[1] first noted that a bubble passing through a liquid-filled tube would move at a velocity higher than the average liquid velocity. In 1942 Landau, Levich[2] and Derjaguin[3] proposed a model for evaluating the thickness of a viscously deposited film as a function of Capillary number ($Ca = \mu U/\sigma$). Later on Bretherton[4] proposed a similar law for a film deposited inside a capillary, valid for thin films and Ca smaller than 0.005. He also found experimentally that aniline ($\theta_{\text{aniline}} = 36°$) does not follow the predicted behavior and the deviation becomes increasingly important as the Capillary number decreases. Teletzke[5] proposed a theory which accounts for the conjoining/disjoining pressure potential to explain the behavior of films thinner than one micron, which cannot alone explain the deviation in Bretherton's data. Aussillous and Quere[6] examined the role of inertia and extended Bretherton's law for higher *Ca*, matching Taylor's experimental data.

Snoeijer[7] showed recently that the thickness of a film coating a plate withdrawn from a liquid reservoir depends on surface wettability. He proved that the film thickness can have two solutions for the partial wetting case. Most notably he found that (Snoeijer[8]) a ridge ending with a shock occurs at the end of a plate deposited film (under partial wetting, $\theta \approx 50°$), which is similar to the experimental findings presented herein. In present experiments a shock was observed during tube film deposition under non-wetting conditions (θ = 105°). Schwartz et. al.[9] examined the infinite and finite bubble in low *Ca* flow and found that the short bubble film obeys Bretherton's law while the long bubble film is almost twice as thick; for intermediate bubble length the film thickness presented multiple solutions possibly due to instabilities. Recently, Herescu and Allen[10] observed that the film thickness increases with the contact angle which might explain the behavior captured in Bretherton's experiments. Changes in film thickness can be brought about by Marangoni stresses which occur at the gas-liquid interface due to the presence of contaminants. There is no general agreement as to what are the conditions when the film thickness increases or decreases and this open interface dynamics problem is yet to find its answers. Marangoni effects on film deposition were studied by Ratulowski[11], Ramdane and Quere[12] as well as Krechetnikov and Homsy[13], to name only a few. In present experiments the film thickness significantly increased for the non-wetting case (105° contact angle) which is believed to be caused by dissipation mechanisms at the moving contact line rather than Marangoni stresses.

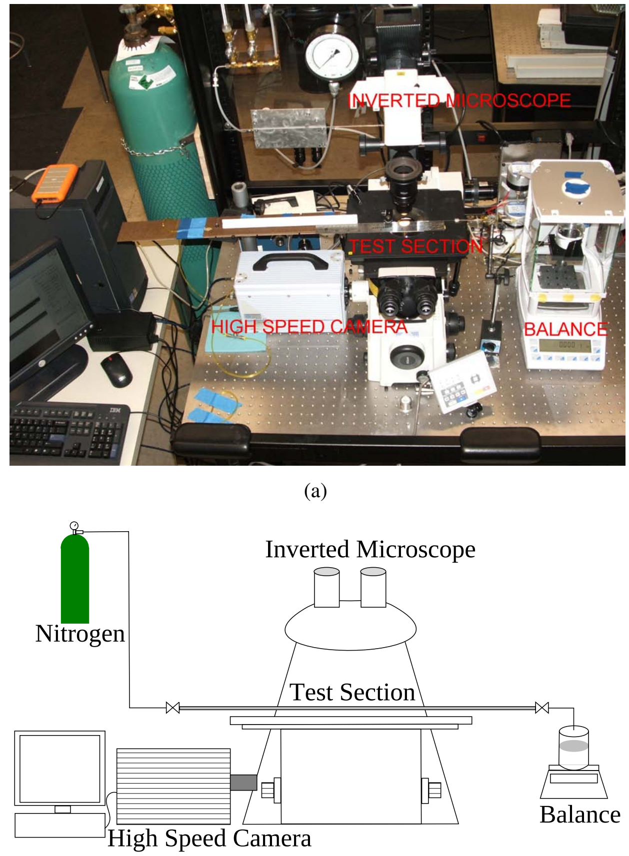

(a)

(b)

Figure 1: Experiment Setup

The Experiment

The experimental setup consisted of a glass capillary tube 12 centimeters long having an internal diameter of 500 microns, a Nikon TE-2000 inverted microscope, a Photron high-speed camera and a Precisa electronic balance (Figure 1). The capillary exit is connected through a valve with rigid tubing which is immersed in the distilled water-filled glass vessel used to contain the expelled liquid. The nonwetting fluoropolymer coating was obtained by passing a Rain-X$^{\text{TM}}$(3M Corporation) liquid slug through the capillary at constant velocity, with the aid of a syringe pump. The coating obtained yields a static contact angle of 105° for water. The experiment begins with the glass tube being filled with distilled water, after which the desired gas pressure is set while keeping the outlet valve closed. When the valve at the test section outlet is opened the filtered compressed nitrogen pushes the liquid out of the capillary while a thin film is left on the wall. The gas-liquid interface dynamics is recorded through the 2X microscope objective at a location 7-8 centimeters downstream of the initial meniscus position, with the aid of the high

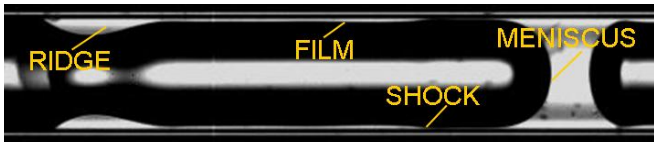

Figure 2: Hydraulic Jump in a Non-Wetting Film

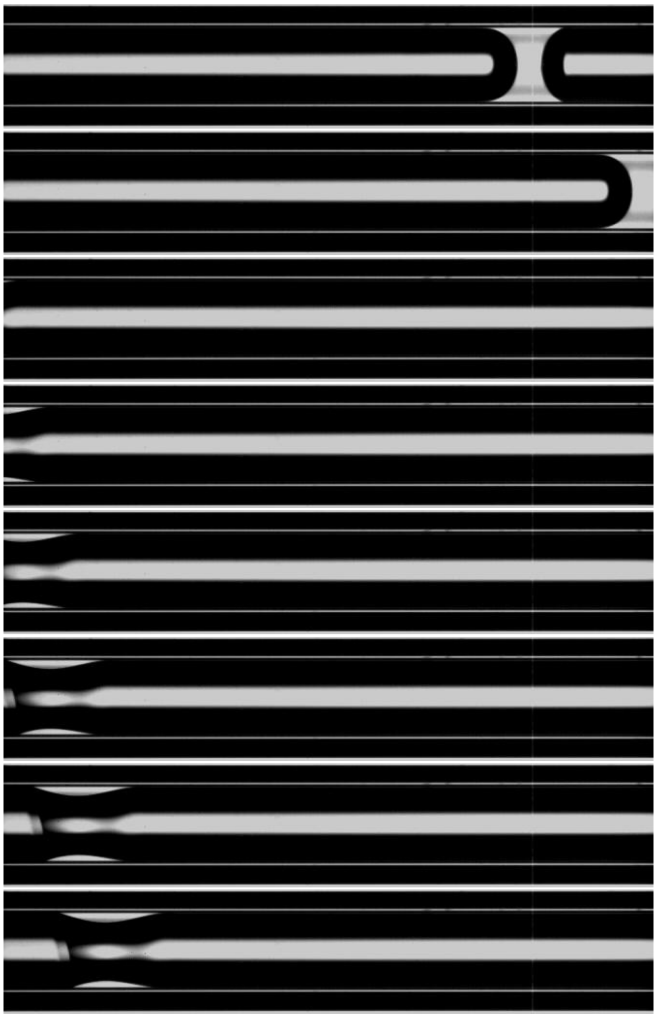

Figure 3: Wetting Taylor bubble , Ca = 0.0034. Images 4 ms apart. The width of the images is 5.735 mm.

speed camera. The experimental error for velocity and length measurements is within 5%.

Experimental Observations

Film deposition experiments were performed with distilled water in a 500 μm glass round capillary, with and without a Rain-

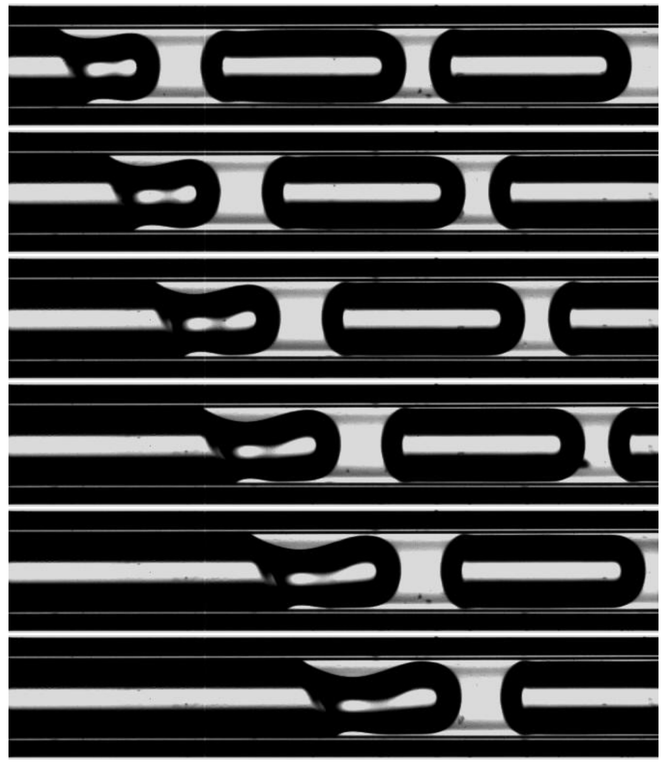

Figure 4: Non-wetting Taylor bubble , Ca = 0.0034. Images 2 ms apart. The width of the images is 5.735 mm.

X coating. A water droplet sitting on the Rain-X coating makes a static contact angle of 105° (*non-wetting*) and a static contact angle of 30° (*wetting*) on a glass surface. When the film is deposited in the glass tube, a Bretherton-Taylor film of uniform thickness is left on the wall. A contrasting behavior has been observed for the film deposited in the Rain-X coated capillary. The film starts thicker than in the uncoated glass capillary case (implicitly thicker than the Bretherton film if we assume the law is valid in a wetting tube) and ends with a ridge, which subsequently grows and forms a plug giving rise to a Taylor bubble flow morphology. If a certain velocity is attained, the film thickness presents an abrupt jump through which the Bretherton film deposited at the meniscus connects with the thicker film merging into the ridge (see Figure 2). The gas bubble appears dark with a bright band along the centerline.The liquid plug, the thin film surrounding the bubble as well as the ridge appear bright with the gas-liquid interface delimiting the dark bubble region. A hydraulic jump (shock) in the film was observed for a number of tests performed in the coated test section, while in the uncoated test section no shock was present in the tested Ca range; for the uncoated channel $0.0018 \leq$ Ca ≤ 0.009 and $0.0024 \leq$ Ca ≤ 0.0069 for the coated. Ca is based on the meniscus velocity.

For both surfaces (wetting and non-wetting) the ridge grows to

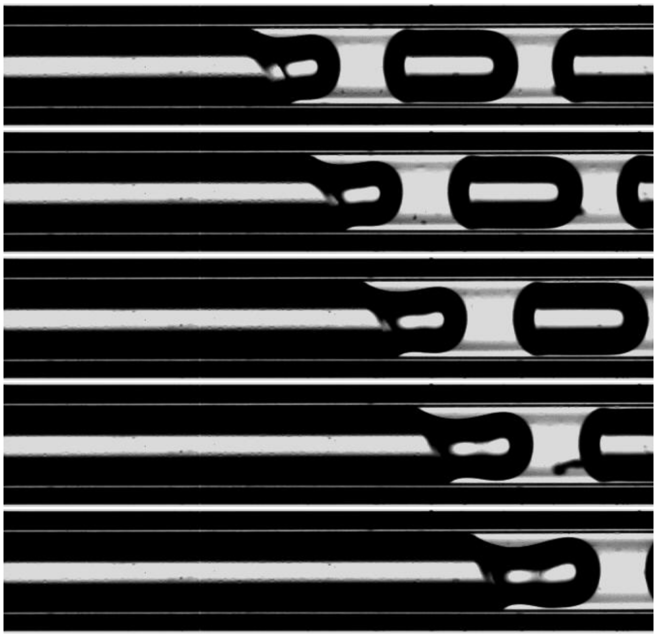

Figure 5: Non-wetting Subcritical Taylor bubble (no shock), Ca = 0.0037. Images 2 ms apart. The width of the images is 5.735 mm.

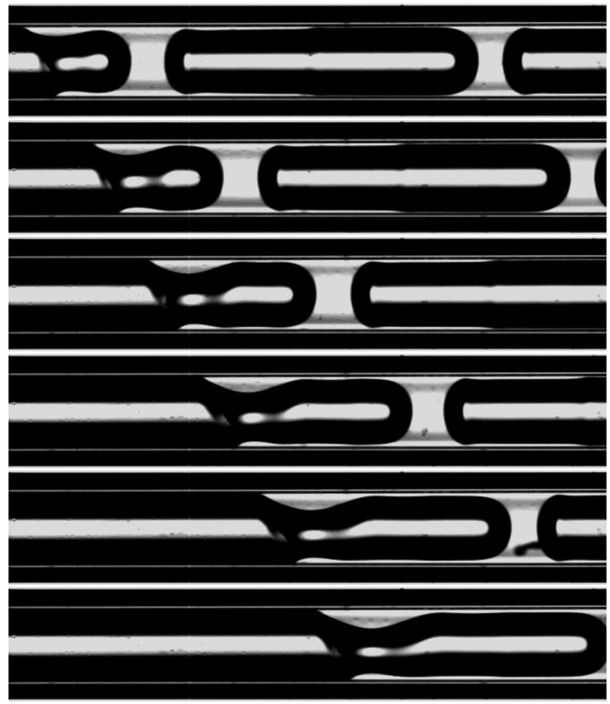

Figure 6: Non-wetting Supercritical Taylor bubble (with shock), Ca = 0.0035. Images 2 ms apart. The width of the images is 5.735 mm.

eventually form a plug and Taylor bubbles. In the bare glass tube, the bubbles are longer than in the Rain-X coated tube. There are also striking differences in the morphology of the deposited film. The non-wetting case presents a hydraulic jump if a critical velocity is exceeded. Below this velocity the shock does not occur and the non-wetting film is thicker than the Bretherton film of the wetting case. Also the bubbles are much shorter in the coated tube. The sequence of images in Figure 3 shows the film deposition in the bare glass tube, a long bubble will eventually form when the ridge grows into a plug. Note the uniform thin film that is laid by the translating meniscus. The capillary number is Ca = 0.0034. On the other hand, if we examine the Taylor bubble in the non-wetting tube at the same Ca we observe that it is considerably shorter than the wetting one (Figure 4). Also, the non-wetting film appears to be thicker than the wetting counterpart.

The shock theory proposed herein states that the critical ridge front velocity U_F necessary for the occurrence of a hydraulic jump is a function of the deposited film thickness. It follows that with increasing Ca the shock cannot form unless the critical U_F is attained. This appears to be supported by the experiments. In Figures 5 and 6 for a Ca greater than a critical value, the shock does not occur if the critical velocity is not reached. In the non-wetting case, the bubble length as well as the film morphology change when a critical velocity is crossed. To exemplify this behavior, we show in Figure 5 a sequence of images taken at Ca = 0.0037 with no shock present. In the same experimental run a shock occurs at Ca = 0.0035 as seen in Figure 6, visible in the formed bubble. Note the shorter bubble length as well as the thicker film for the sub-critical case (no shock). The film thickness presents a jump when a critical state is reached (shock). The non-axisymmetric ridge is caused by an azimuthal instability, more likely to occur in the non-wetting deposition.

Discussion

Hydraulic Jump in a Non-Wetting Film

The ridge is connected to the liquid meniscus through a film which presents an abrupt change in thickness once a critical state is attained (Figure 7). We hypothesize that the transition in film thickness occurs through a hydraulic jump (shock) which can subsequently be characterized by writing the conservation of mass and momentum across the shock. The liquid film from the ridge side has a velocity V_1 and flows over a stagnant film (Figure 8(a)), while the wave front travels at a velocity c. In a reference frame translating with c, the film deposited by the meniscus (thickness e) enters the shock with a velocity V_1 which changes to $c - V_1$ after the jump (Figure 8(b)).

The following hypotheses are made when the conservation of mass and momentum are written across the shock:

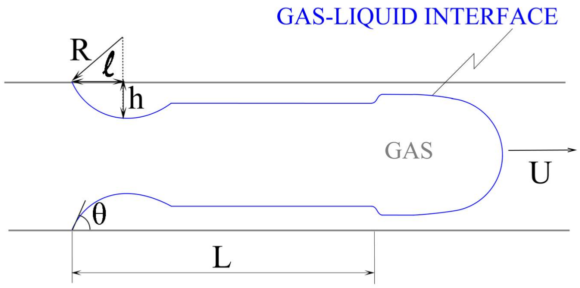

Figure 7: Non-Wetting Film Deposition with Hydraulic Jump

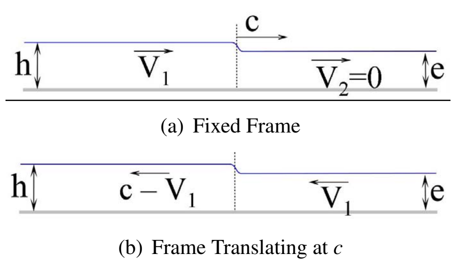

Figure 8: Hydraulic Jump in a Non-Wetting Film

1. Wall shear and shear at the gas-liquid interface are neglected
2. The interface curvature gradient between the ridge and the film laid by the meniscus is driving the shock
3. The azimuthal curvature is neglected

Conservation of mass:

$$V_1 e = (c - V_1)\, h \tag{1}$$

Conservation of momentum:

$$-\rho\left[-c^2 e + (c - V_1)^2 h\right] = \Delta P \cdot h \tag{2}$$

The pressure change across the ridge's interface can be written, neglecting the azimuthal curvature, as $\Delta P = \sigma/R$ (Laplace equation). The geometrical interdependence between the dynamic contact angle θ, the height h and the radius of curvature R of the ridge, and the ridge half-width l (depicted in Figure 7) can be written as:

$$\sin\theta = l/R \tag{3}$$

and

$$h = R - \frac{l}{\tan\theta} \tag{4}$$

From mass continuity, momentum, the Laplace equation and the geometrical relations at the ridge it can be concluded that the wave front velocity varies as:

$$c^2 = \frac{\sigma}{e\rho}(1 - \cos\theta)\frac{(e+h)^2}{(e+h)^2 - eh} \tag{5}$$

The critical velocity necessary to have a shock is reached when $e = h$:

$$V_c^2 = \frac{4\sigma}{3e\rho}(1 - \cos\theta) \tag{6}$$

If $V_1 > V_c$ the film deposited by the meniscus will connect to the ridge through a hydraulic jump.

The wave front velocity U_F is plotted in Figure 9 as a function of the deposited film thickness h_R (e non-dimensionalized by the tube radius) for both coated and uncoated test sections. h_R dependency on Ca is given as a correlation in [6]. The data points where a shock was observed are marked with an "S". The Froude critical velocity([14]), the inertial dewetting limit([14]) as well as the shock prediction proposed for an interface curvature gradient driven shock are shown as curves. Critical velocity lines above which a shock should occur according to Eqn 6 are shown for dynamic contact angles of θ_d = 5°, 7° and 10°. $U_{F,nonwet}$, $U_{F1,nonwet}$ and $U_{F2,nonwet}$ represent wave front velocities measured a week apart in three separate runs with the coated test section, to check for repeatability and coating degradation. A hydraulic jump (shock) in the film was observed for a number of tests performed in the coated test section, while in the uncoated (denoted as $U_{F,wet}$) no shock was present in the tested Ca range. For the uncoated section 0.0018≤ Ca ≤0.009 and for the coated the tests were in the interval 0.0024≤ Ca ≤0.0069.

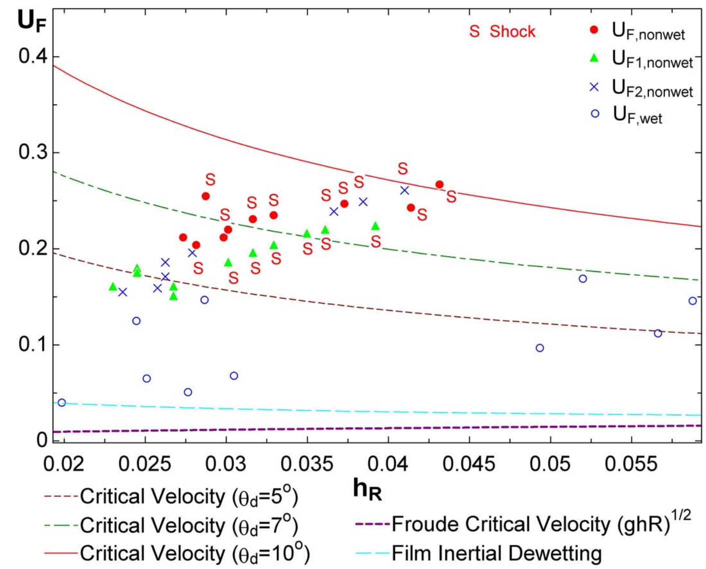

Figure 9: Front Velocity vs. Nondimensional Film Thickness. $U_{F,nonwet}$, $U_{F1,nonwet}$ and $U_{F2,nonwet}$ are wave front velocities measured in three separate runs with the non-wetting test section. $U_{F,wet}$ is taken in the wetting tube.

The Froude shallow water wave theory nor the inertial dewetting assumption can explain the shock manifestation. If a dynamic contact angle of $\theta_d = 6°$ is considered in the proposed theory for the critical velocity according to Eqn. 6, it can be inferred that above V_c a shock should occur as observed in the experiments. This hypothesis does not exclude a Ca cutoff, a transition capillary number might also exist in the interval 0.0031 $\leq$ Ca $\leq$ 0.0035.

Emerging Scales

As previously mentioned, a transition Ca may exist having a value around 0.0034 for the Rain-X coated test section. The presence of a shock can be attributed to the contact line dynamics, which makes a dynamic contact angle as it translates and also sets the curvature of the ridge. The interface curvature gradient is different for the non-wetting and wetting tubes and it is believed to cause the shock formation in the coated non-wetting test section. The contact line velocity for the non-wetting case was measured in three different experimental rounds and it is presented in Figure 10. Notably near the transition capillary number, U_{CL} presents multiple solutions which indicates that the occurrence of the critical regime (shock formation) is intimately connected to the contact line behavior. If we look at the first data set (red dots) we can see that multiple U_{CL} exist at Ca = 0.0034, and at the same time the smallest Ca at which a shock was observed is

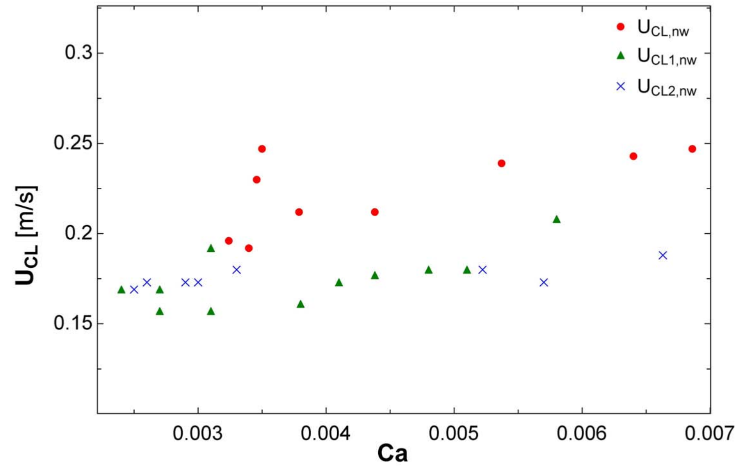

Figure 10: Contact Line Velocity vs. Ca. $U_{CL,nw}$, $U_{CL1,nw}$ and $U_{CL2,nw}$ are contact line velocities measured in the non-wetting tube in three test runs.

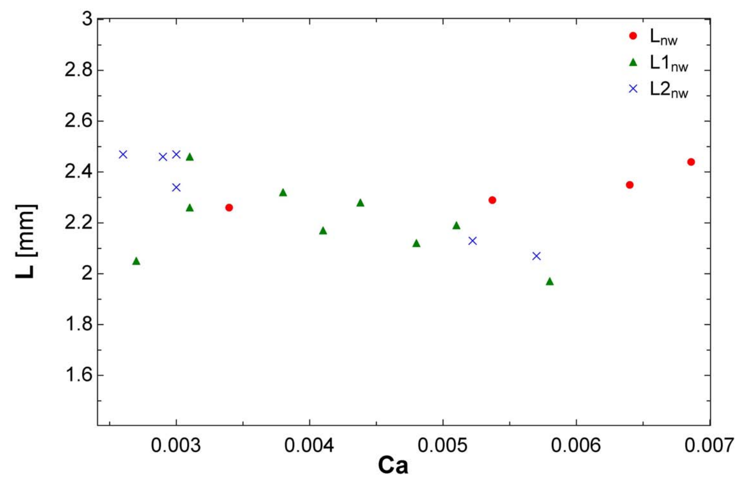

Figure 11: Transition Length vs. Ca. L_{nw}, $L1_{nw}$ and $L2_{nw}$ represent the distance between the contact line and the hydraulic jump when first observed (measured in three test runs).

0.0035.

The bubble length and film thickness also present a behavior which is closely related to the existence of the shock. Short Taylor bubbles with a thicker film are formed as long as there is no shock, while if a shock occurs the bubbles are longer with a thin film at the meniscus and a thicker film towards the ridge. The distance L between the contact line and the location where the shock is first observed is plotted as a function of Ca in Figure 11. This length appears to be independent of the capillary number and it can be regarded as a cutoff bubble length above which a shock will occur.

Perhaps the most notable mechanism which could cause the observed hydraulic jump apart from the assumed contact line dynamics mechanism is contamination. Marangoni stresses can in principle cause a film thickening but it is less clear why the shock occurs as the velocity increases, when surface tension gradients are expected to lessen in importance. The capillary number of 0.0035 at which the shock was noted is rather high, the contamination effects are usually visible at much lower values. To better understand this issue, experiments were performed in Teflon tubing and the same behavior was observed with a shock occurring above a critical velocity.

Film thickening for low viscosity fluids due to inertia has been investigated by Aussillous and Quere[6] who proposed a critical Capillary number Ca* above which inertial effects become noticeable. In present experiments the maximum Ca is 0.009 while Ca* $\approx$ 0.01 therefore inertial effects are not expected to increase the film thickness or play a part in the shock formation.

Conclusion

Film deposition experiments performed in wetting and non-wetting tubes revealed the presence of a ridge bound by a moving contact line, at the downstream end of of the laid film. The dynamics of the ridge was investigated and it was noted that the front and contact line velocities of the non-wetting structure are larger than those of the wetting counterpart. It is believed that the differing contact line dynamics for the two surfaces (wetting and non-wetting) cause a series of morphological changes in the Taylor bubbles that form during the flow. The wetting bubbles are much longer than the non-wetting ones, the latter presenting a thicker film. During the deposition of the non-wetting film a shock was observed when a critical velocity is attained. A relation for the critical velocity was derived assuming that the shock is driven by the curvature gradient between the ridge and the deposited film. A critical capillary number of 0.0035 above which the shock occurs may also exist. Short Taylor bubbles with a thicker film are formed as long as there is no shock, while if a shock occurs the bubbles are longer with a thin film at the meniscus and a thicker film towards the ridge. It is remarkable that the distance L between the contact line and the location where the shock is first observed appears to be independent of the capillary number. It follows as well that L can be regarded as a cutoff bubble length above which a shock will occur. It is most likely a relevant scale to the observed phenomenon and future investigation is necessary to determine the appropriate physical interplay.

REFERENCES

[1] F. Fairbrother and A. E. Stubbs. Studies in electro-endosmosis. part vi. the bubble-tubemethod of measurement. *J. Chem. Soc*, 1:527529, 1935.

[2] L. Landau and B. Levich. Dragging of a liquid by a moving plate. *Acta Physicochim. USSR*, 17:4254, 1942.

[3] B. V. Derjaguin. On the thickness of a layer of liquid remaining on the walls of vessels after their emptying, and the theory of the application of photoemulsion after coating on the cinefilm. *Acta physico-chemica USSR*, 20:349–352, 1943.

[4] F. P. Bretherton. Motion of long bubbles in tubes. *Journal of Fluid Mechanics*, 10(Part 2):166–188, 1961.

[5] G. F. Teletzke. *Thin liquid films: molecular theory and hydrodynamic implications*. PhD thesis, University of Minnesota, 1983.

[6] P. Aussillous and D. Quere. Quick deposition of a fluid on the wall of a tube. *Physics of Fluids*, 12(10):2367–2371, 2000.

[7] J. H. Snoeijer, J. Ziegler, B. Andreotti, M. Fermigier, and J. Eggers. Thick films of viscous fluid coating a plate withdrawn from a liquid reservoir. *Physical Review Letters*, 100 (24), 2008.

[8] Jacco H. Snoeijer, Giles Delon, Marc Fermigier, and Bruno Andreotti. Avoided critical behavior in dynamically forced wetting. *Physical Review Letters*, 96(17):174504, 2006.

[9] L. W. Schwartz, H. M. Princen, and A. D. Kiss. On the motion of bubbles in capillary tubes. *Journal of Fluid Mechanics Digital Archive*, 172(1):259–275, 1986.

[10] Alexandru Herescu and Jeffrey S. Allen. The effect of surface wettability on viscous film deposition. Proceedings of the 7th International ASME Conference on Nanochannels, Microchannels and Minichannels, ICNMM2009, Pohang, Korea, 2009.

[11] J. Ratulowski and H. C. Chang. Marangoni effects of trace impurities on the motion of long gas bubbles in capillaries. *Journal of Fluid Mechanics Digital Archive*, 210(-1):303–328, 1990.

[12] O. O. Ramdane and D. Quere. Thickening factor in marangoni coating. *Langmuir*, 13(11):2911–2916, 1997.

[13] R. Krechetnikov and G. M. Homsy. Surfactant effects in the landaulevich problem. *Journal of Fluid Mechanics*, 559: 429–450, 2006.

[14] P. G. De Gennes, F. Brochard-Wyart, D. Quere, and A. Reisinger. *Capillarity and wetting phenomena: drops, bubbles, pearls, waves*. Springer Verlag, 2004.

Acknowledgements

This work was partially supported by NSF CBET-0748049, DOE DE-FG36-07GO17018 and by the Department of Mechani-

cal Engineering - Engineering Mechanics at Michigan Tech University.